An attractive agro-industrial by-product in environmental cleanup: Dye biosorption potential of untreated olive pomace

Tamer Akar [a,*], Ilknur Tosun [a], Zerrin Kaynak [b], Esra Ozkara [a], Onur Yeni [a], Esin N. Sahin [a], Sibel Tunali Akar [a]

[a] Department of Chemistry, Faculty of Arts and Science, Eskişehir Osmangazi University, Campus of Meselik, 26480 Eskişehir, Turkey
[b] The Program of Chemistry, Vocational School of Higher Education, Bilecik University, 11210 Bilecik, Turkey

ARTICLE INFO

ABSTRACT

This research deals with the evaluation of highly available and cost effective waste biomass of olive pomace for the removal of reactive textile dye, RR198 from aqueous medium and a real effluent. The experiments were conducted to assess the effects of process variables such as initial pH, biosorbent dosage, contact time, temperature and ionic strength. The results showed that the highest dye biosorption capacity was found at pH 2 and the needed time to reach the biosorption equilibrium was 40 min with a biosorbent concentration of $3.0\,\mathrm{g\,L^{-1}}$. The sorption kinetics of dye was best described by the pseudo-second-order kinetic model. The equilibrium biosorption data were analyzed by Langmuir, Freundlich and Dubinin–Radushkevich isotherm models and the results from the isotherm studies showed that the RR198 biosorption process occurred on a homogenous surface of the biosorbent. The waste biomass of olive oil industry displayed biosorption capacities ranging from 6.05×10^{-5} to $1.08 \times 10^{-4}\,\mathrm{mol\,g^{-1}}$ at different temperatures. The negative values of ΔG° and the positive value of ΔH° suggest that the biosorption process for RR198 was spontaneous and endothermic. Dye–biosorbent interactions were examined by FTIR and SEM analysis. Finally, high biosorption yield of olive waste for the removal of RR198 dye from real wastewater makes it possible that the olive pomace could be applied widely in wastewater treatment as biosorbent taking into account that no pretreatment on the solid residue is carried out.

© 2008 Elsevier B.V. All rights reserved.

1. Introduction

The olive oil industry has a great economical importance in many Mediterranean countries, i.e., Spain, Italy, Greece, Turkey, Tunisia and Morocco [1,2]. It is estimated that there are approximately 95 million olive trees and 658,000 ha olive orchard in Turkey [3]. The annual production of olive oil in Turkey is 100,000–250,000 tons [4]. Olive oil is produced from olives using hydraulic presses or modern horizontal axis centrifuges and both processes generate highly polluted wastewater and/or solid residue [5,6]. The solid waste is commonly known as "olive cake" or "olive pomace" [7]. Olive pomace consists of cellulose, lignin, amino acid, protein and uronic acids along with oily wastes and polyphenolic compounds. These components contain many functional groups. These include carboxylic, hydroxylic and methoxy groups and a high amount of fixed anionic and cationic functional groups [8,9]. The pomace is generally swallowed by means of controlled spreading on agricultural soil. Only small amount of this residue is used as natural fertilizer, a source of heat energy and additive in animal food [10]. Most of these applications are not believed to have great economical value [11]. Therefore it would be beneficial to find other applications for such an agro-industrial solid waste.

Although olive pomace has no market value, the use of this substance or its by-products as adsorbent for some heavy metal ions [7,9,11,12–14] is limited. There is lack of information about the sorption ability of untreated olive pomace for the removal of reactive dyes. Therefore, it is chosen as sorbent material in this study. To our knowledge, olive pomace is only used to prepare active carbon as adsorbent to remove methylene blue [10,15–17] and RR22 [18] apart from the degradation of Azo-dye orange (II) [19].

Approximately 10,000 different dyes are commercially available and annual production of dyes is more than 7×10^5 metric tones worldwide [20]. Textile dye effluents contain reactive dyes in a concentration range of $5–1500\,\mathrm{mg\,L^{-1}}$. Therefore, the treatment of dye contaminated effluents is currently a primary environmental concern [21]. Generally, sorptive processes can reduce capital, operational and total treatment costs by 20%, 36% and 28%, respectively, when compared with the conventional processes [12]. In recent years, a number of studies have focused on the use of different potential agricultural materials as inexpensive adsorbents for the removal of dyes from aqueous solutions. Some of these are de-oiled soya waste [22], sunflower seed hull [23], baggase pith [24], banana

* Corresponding author. Tel.: +90 222 239 3750/2871; fax: +90 222 2393578.
E-mail address: takar@ogu.edu.tr (T. Akar).

and orange peels [25], sugar cane dust [26] and raw date pits [27], *Phaseolus vulgaris* waste [28]. But new, economical, easily available and highly effective adsorbents are still needed. This study provides such information and aims to reverse the current negative human activities and use solid agro-industrial waste, olive pomace, for environmental cleanup from reactive dye pollution.

The objective of the present study was to conduct a preliminary study on the use of olive pomace as reactive dye biosorbing material. The solid waste was characterized using FTIR and SEM analysis. In order to determine the surface charge of waste biomass, zeta potential measurements were carried out. Reactive Red 198 (RR198) was selected as a model sorbate due to its extensive use in textile industry. The biosorption experiments were conducted in various operating conditions (such as pH, biosorbent dosage, time, ionic strength and temperature). The biosorption mechanism was investigated using the pseudo-first-order, the pseudo-second-order and intraparticle diffusion kinetic models and some thermodynamic constants were calculated. Equilibrium biosorption data were analyzed by Langmuir, Freundlich and Dubinin–Radushkevich (D–R) isotherm models. In order to evaluate the potential use of olive pomace in industrial wastewater, the proposed biosorption process was also applied to real samples.

2. Material and methods

2.1. Preparation of the biosorbent

Biosorbent material was the solid waste of olive oil production, provided from Gemlik, Turkey. The sample was repeatedly washed with deionized water to remove adhering dirt and soluble impurities and dried at 80 °C, to obtain a constant weight. Next, it was crushed and sieved, using an ASTM Standard sieve, to select the particle sizes of less than 150 μm. The powdered biosorbent was stored in a glass bottle prior to use in biosorption studies.

2.2. RR198 solutions

The textile dye, RR198, was obtained from a local textile factory and selected as a representative reactive dye for this study. Its chemical structure is shown in Fig. 1. RR198 was dissolved in deionized water to prepare the stock solution with required concentration of 1000 mg L^{-1}. The concentrations of RR198 used in this study (50–500 mg L^{-1}) were obtained by dilution of the stock solution. The pH of the solution was adjusted to the desired value by adding a small quantity of 0.1 mol L^{-1} HCl, and/or 0.1 mol L^{-1} NaOH.

2.3. Experimental operations

Batch experiments were conducted in 100 mL glass beakers containing known concentrations of RR198 solutions. The effect of pH on the biosorption process was examined by equilibrating the mixture containing 0.1 g of biosorbent samples, and RR198 solutions were used at a concentration of 100 mg RR198 L^{-1}, with pH values ranging from 1 to 10. The mixture was stirred at 200 rpm for 60 min using a digitally controlled magnetic stirrer. The samples
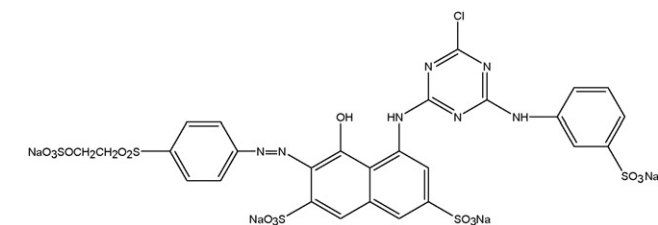
were centrifuged at 4500 rpm for 3 min in order to separate the solid phase from the liquid phase. The supernatants were analyzed for the determination of the remaining RR198 concentration by a spectrophotometer. In order to predict the effect of the biosorbent dosage on the removal of RR198, biosorbent concentration was varied between 0.4 and 4.0 g L^{-1}, at the optimum solution pH of 2.0. The biosorption kinetics of RR198 was examined at constant temperatures of 20, 30, 40 and 50 °C and the contact time ranged from 5 to 90 min. The pseudo-first-order, the pseudo-second-order and intraparticle diffusion kinetic models were applied to data. The effect of salt concentration was investigated. The Langmuir, Freundlich and D–R isotherm models were examined in batch mode using an initial RR198 concentration range of 50–500 mg L^{-1} and varying operating temperatures. In addition, the thermodynamic parameters of biosorption were extracted using the Langmuir isotherm constant (K_L). The biosorption capacity (q_e) of olive pomace was calculated from the following general mass-balance equation:

$$q_e = \frac{V(C_i - C_e)}{m} \tag{1}$$

where C_i and C_e represent the initial and equilibrium concentrations of RR198, respectively, V is the volume of the dye solution (L) and m is the amount of olive pomace (g).

2.4. Instrumentation

All pH measurements were carried out with a WTW INOLAB 720 model digital pH meter. A Shimadzu UV-2550 model UV/vis spectrophotometer equipped with a tungsten lamp was used to determine the dye concentrations in the solutions at λ_{max} 515 nm. FTIR spectra of unloaded and dye-loaded biosorbent were recorded in a PerkinElmer Spectrum 100IR infrared spectrophotometer in the region of 400–4000 cm^{-1}. The samples were prepared as KBr pellets under high pressure. The surface structure and morphology of the biosorbent material before and after dye biosorption were characterized using a scanning electron microscope (JEOL 560 LV SEM), at 20 kV and a 1000× magnification. Prior to analysis, the samples were coated with a thin layer of gold under an argon atmosphere to improve electron conductivity and image quality. The surface charge characteristics of the biomass at different pH values were determined from Zeta potential measurements by a Zetasizer (Malvern Zetasizer nano ZS).

2.5. Real wastewater application

The wastewater sample was collected from a local factory in Eskişehir, Turkey. The sample was placed in a sterile container, transferred to the laboratory, and stored at 5 °C. In order to investigate the matrix effect on the biosorption capacity of waste biomass, the experiments were carried out with spiked wastewater samples with RR198. The spiked samples were prepared by including RR198 dye at concentrations ranging from 5 to 150 mg L^{-1}. The application of the proposed biosorption method was investigated under the predetermined optimum conditions. The biosorption yield was calculated by using the following equation:

$$\text{Biosorption yield} (\%) = \frac{C_i - C_e}{C_i} \times 100 \tag{2}$$

3. Results and discussion

3.1. Characterization of olive pomace

Olive pomace used in this study was analyzed by scanning electron microscopy in order to examine its morphology. SEM image of fracture surface of unloaded biomass is shown in Fig. 2(a), and indicates the porous structure of the biomass. The biosorbent has some
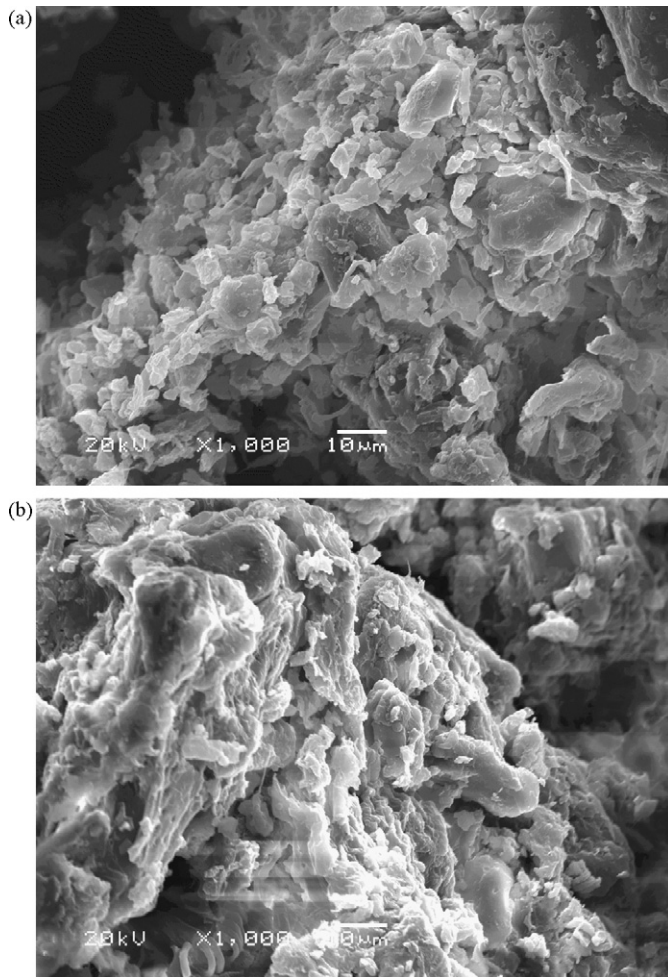
Fig. 1. Chemical structure of RR198.

(a)

(b)

Fig. 2. SEM micrograph of (a) olive pomace and (b) RR198-loaded olive pomace.

cavities on the external surface capable of uptaking dye molecules. This structural feature of the biomass may be important since it increases the total surface area [29]. Fig. 2(b) shows that the biomass structure changed upon sorbing the RR198, and had a tendency to form agglomerates [30]. The differences in the surface morphology of untreated and RR198 treated-olive pomace clearly confirm the presence of the dye molecules on the waste biomass.

The FTIR spectra of unloaded and RR198 loaded biomass in the range of 400–4000 cm^{-1} were taken in order to find out which functional groups are responsible for the biosorption process and presented in Fig. 3. This figure (a) reflects the complex nature of the unloaded biomass with a number of absorption peaks. It has previously reported that all of the biological sorbent materials have intense absorption bands around 3500–3200 and 1540 cm^{-1} which represent the stretching vibrations of amino groups. These bands are superimposed onto the side of the hydroxyl group band at 3500–3300 cm^{-1} [29]. A similar and very strong absorption peak was observed for unloaded biomass at about 3428 cm^{-1}. There was an important intensity decrease in the same peak for dye-loaded biomass. Absorption band at 1540 cm^{-1} also disappeared after the biosorption of RR198. The spectrum of unloaded biomass also displays absorption peaks at about 2924 and 2852 cm^{-1}, corresponding to stretching of C—H bonds of methyl and methylene groups present in the lignin structure [31]. There was a sharp increase in intensity of these absorption bands observed at same frequencies in the spectrum of dye-loaded biomass due to the biosorption of reactive dye molecules including different C–H groups in its chemical structure. The carboxyl groups showed a
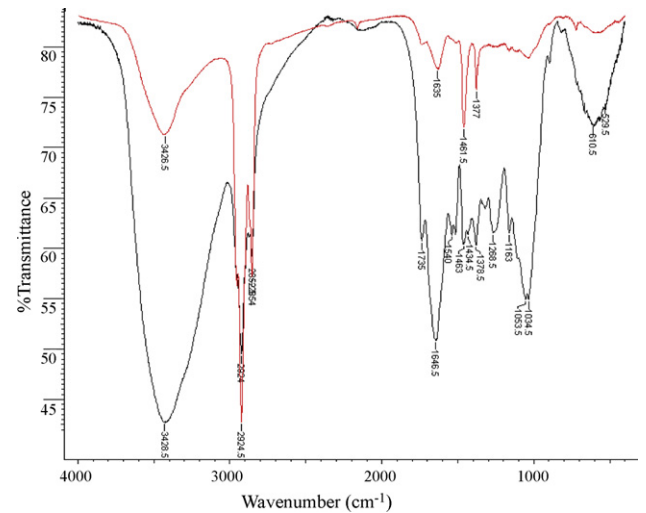

Fig. 3. FTIR spectra of (a) olive pomace and (b) RR198-loaded olive pomace.

characteristic absorption peak at 1646 cm^{-1} for unloaded biomass, and this band shifted to a lower frequency (1635 cm^{-1}) with a significant decrease in intensity after dye biosorption. The disappearance of stretching bands of aromatic ring (1434 cm^{-1}) and C–O (1034 cm^{-1}) groups of lignin after biosorption process may be related to an interaction between the dye molecules and the lignin structure on the biomass surface. The band at about 1268 cm^{-1} that corresponded to bending vibrations of O–C–H, C–C–H and C–O–H groups [31] disappeared in the FTIR spectrum of the dye-loaded biomass. The absorption peaks around 1163 and 1053 cm^{-1} are indicative of P–O stretching and P–OH stretching vibrations, respectively [32]. The band between 610 and 530 cm^{-1} for unloaded biosorbent represents C–N–C scissoring that is only found in protein structures [29] and this band disappeared after RR198 biosorption onto solid waste.

It can be noted that the FTIR spectrum of unloaded biomass supports the presence of amine groups and this is likely to be responsible for RR198 biosorption. Carboxyl and phosphate groups may electrostatically inhibit the binding of RR198 at high pH value of 3.0 [33]. The changes observed in the spectra indicated the possible involvement of functional groups in the biosorption process on the surface of the biomass.

The surface charge of the biomass determined by measuring the zeta potential of its suspension varied from +5.12 to −13.20 mV with the corresponding pH change from 1.0 to 10.0 (Fig. 4). The surface charge on the biomass is predominantly positive at pH 1.0–2.0 due to protonation of functional groups such as amines. These groups
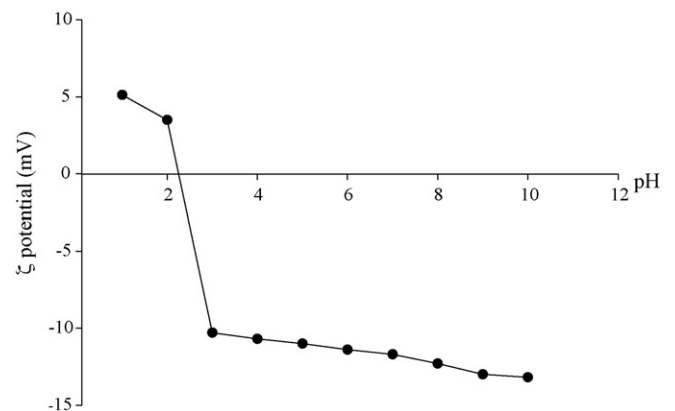

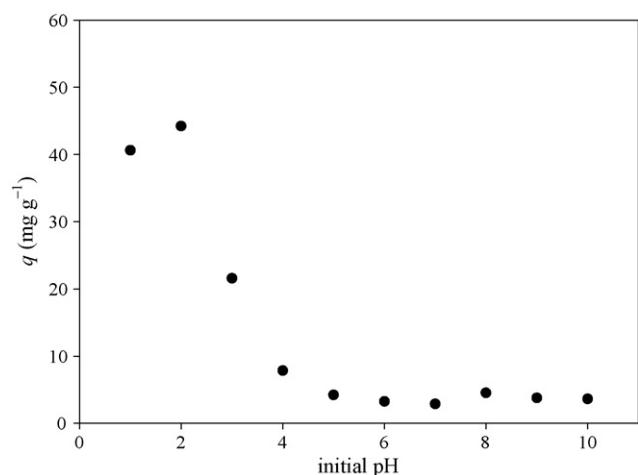**Fig. 4.** ζ potentials of olive pomace at different pH values.

Fig. 5. Effect of initial pH on the biosorption of RR198 onto olive pomace.

may be the major biosorption sites for anionic dye removal. Above pH 2.0 net negative charge density on the biomass increased due to deprotonation of carboxylate and phosphate groups [34].

3.2. Effect of initial pH

Previous studies on dye removal indicated that solution pH has significant effect on the surface charge of the biosorbent and ionization degree of dye molecules. Since pH is one of the important parameters affecting the biosorption ability of biomass, optimum pH was determined for the biosorption of RR198 onto olive pomace. The results are depicted in Fig. 5. This figure indicates that an increase in the initial pH of the medium has a negative effect on dye removal capacity of biomass. According to Fig. 4 the overall surface charge of the biomass was positive upto ~pH 3.0. Anionic dye molecules would be expected to interact more strongly with the positively charged functional groups on the biomass surface. Therefore maximum biosorption capacity was found to be 44.23 mg g^{-1} at the optimum pH value of 2.0. As the pH is increased, the surface charge on the biomass surface will become negative and thus the biosorption capacity of olive pomace will sharply decrease.

3.3. Effect of biosorbent dosage

The effect of biosorbent concentration on RR198 biosorption is illustrated in Fig. 6. The percentage biosorption yield increased
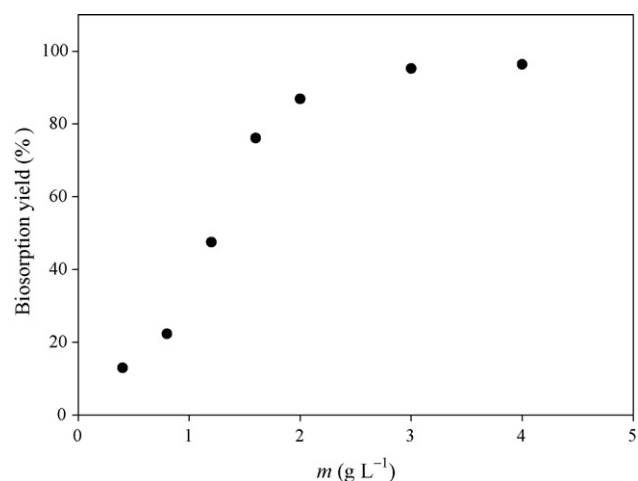

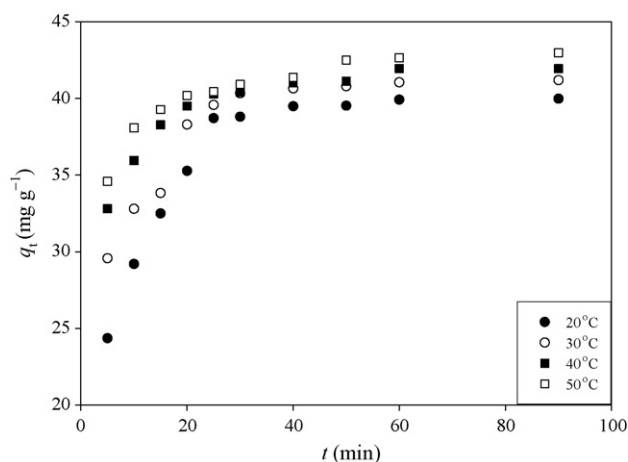**Fig. 6.** Effect of biosorbent dosage on the biosorption of RR198 onto olive pomace.

Fig. 7. Equilibrium time profile for the biosorption of RR198 onto olive pomace at different temperatures.

from 13.00 to 95.24% with an increase in the biosorption dosage from 0.4 to 3.0 g L^{-1}. An increase in the biosorption yield with the biosorbent dosage may be attributed to the increased surface area of the biomass and the number of possible binding sites [35,36]. When the biosorbent dosage was increased to 4.0 g L^{-1}, the biosorption yield was almost constant, due to saturation of the biosorbent surface with RR198 molecules [37]. Therefore, the optimum biomass concentration was selected as 3.0 g L^{-1} for the further experiments.

3.4. Effect of contact time and temperature

Fig. 7 shows the time dependency of RR198 biosorption capacity of biomass at temperatures of 20, 30, 40 and 50 °C. The results clearly indicate that the biosorption process on the waste biomass completed within 40 min and beyond which the curves became flattened. The equilibrium biosorption capacity of olive waste increased from 39.49 to 41.37 mg per gram weight of biosorbent when the temperature was increased from 20 to 50 °C. After this period, dye biosorption was virtually constant due to establishment of the biosorption equilibrium. The equilibrium biosorption capacity of olive pomace for RR198 was favored at higher temperature. The observed trend in increased biosorption capacity with increasing temperature suggests that the biosorption of RR198 dye by waste biosorbent is kinetically controlled by an endothermic process.

3.5. Effect of ionic strength

For a good approximation of the experimental data to the real situation, effluents with salt needed to be treated. Therefore, tests were performed with solutions at different ionic strengths. Ionic strength of the solutions was adjusted with NaCl. The effect of sodium chloride concentration on dye uptake was studied with the variation of NaCl concentration from 0.01 to 0.30 mol L^{-1}. The results are shown in Fig. 8. It is clear that the biosorption of RR198 onto olive pomace is independent of ionic strength in the concentration range of 0.01–0.15 mol L^{-1}. However, an increase in the ionic strength over 0.15 mol L^{-1} results in a decrease in RR198 removal capacity of biomass about 6.65%. It was reported that generally, the biosorption mechanism of surface complexation is pH-dependent, whereas ion-exchange is ionic strength-dependent [38,39]. The ionic strength-dependent and -independent biosorption trend at different NaCl concentrations may be explained by both surface complexation and ion exchange mechanisms for RR198 biosorption.
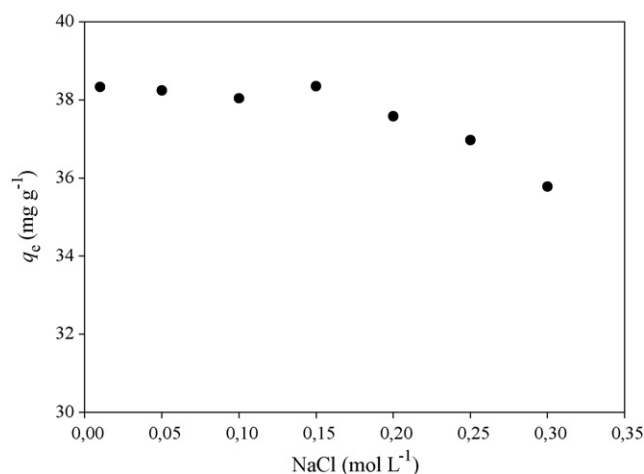
Fig. 8. Effect of ionic strength on the biosorption of RR198 onto olive pomace.

Fig. 9. Pseudo-second-order kinetic plots for the biosorption of RR198 onto olive pomace at different temperatures.

3.6. Kinetic study of biosorption

In order to determine the time required to attain the biosorption equilibrium, kinetic experiments are necessary [40]. The several kinetic models are used to examine the biosorption mechanism such as mass transfer and chemical reaction. One of them is Lagergren's pseudo-first-order model and it assumes that the occupation rate of biosorption sites is proportional to the number of unoccupied sites [41,42]:

$$\ln(q_e - q_t) = \ln q_e - k_1 t \tag{3}$$

where q_e and q_t are the amount of biosorbed RR198 on the biosorbent at equilibrium and at time t (mg g^{-1}), respectively. k_1 is the pseudo-first-order rate constant (min^{-1}). k_1 and q_e values were calculated from the slope and intercept, respectively, of the plot of $\ln(q_e - q_t)$ versus t (figure not shown). The model constants were presented in Table 1. r^2 values are reasonably low and the calculated q_e values obtained from this kinetic model do not give reasonable values. Therefore, it can be suggested that the RR198 biosorption process was not a first-order reaction.

Ho's pseudo-second-order kinetic model has been extensively used by a great number of authors due to its simplicity and the reasonable representation of experimental data [40]. The model equation [43] is:

$$\frac{t}{q_t} = \frac{1}{k_2 q_2^2} + \frac{1}{q_2} t \tag{4}$$

where k_2 is the rate constant of pseudo-second-order kinetic model (g mg^{-1} min^{-1}). Values of k_2 and q_2 were calculated from a plot of t/q_t against t (Fig. 9). r^2 values are reasonably high at all temperatures studied and the calculated q_e values obtained from this kinetic model agree with the experimental values (Table 1). Therefore, the pseudo-second-order model was able to fit with accuracy of the whole experimental data, indicating that the rate-limiting step is a chemical biosorption process.

When the biosorbent is treated as a porous material in aqueous solution, the diffusion process can affect the biosorption process [44]. The pseudo-first-order and pseudo-second-order kinetic
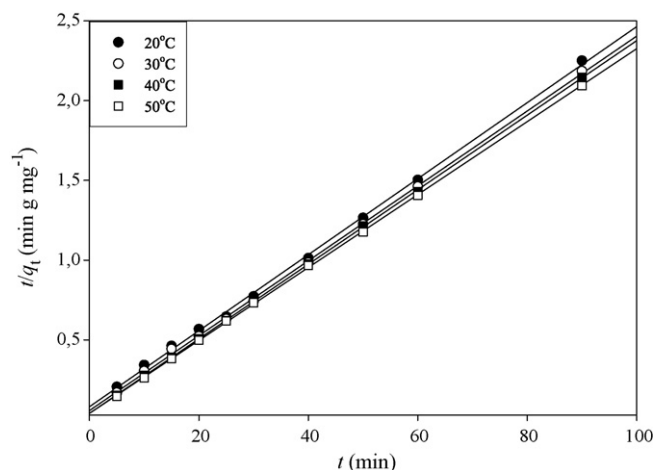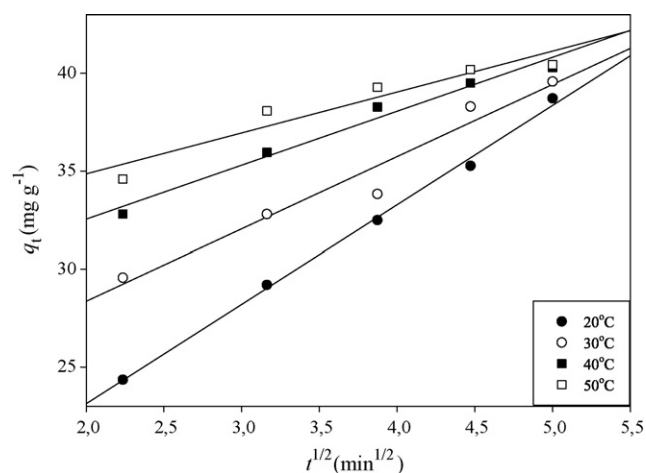

Fig. 10. Intraparticle diffusion kinetic plots for the biosorption of RR198 onto olive pomace at different temperatures.

models could not identify the diffusion mechanism. Therefore, the intraparticle diffusion equation was applied to examine the intraparticle diffusion mechanism as the rate-limiting step in RR198 biosorption. The equation is given as:

$$q_t = k_p t^{1/2} + C \tag{5}$$

where C is the intercept and k_p is the intraparticle diffusion rate constant (mg g^{-1} min$^{-1/2}$). According to this model, the plot of uptake, q_t, versus the square root of time, $t^{1/2}$, (Fig. 10), should be linear if intraparticle diffusion is involved in the biosorption system and if these lines pass through the origin, then intraparticle diffusion is the rate controlling step [45–49]. When the plots do not pass through the origin, this is indicative of some degree of boundary layer control and this further indicates that the intraparticle diffusion is not the only rate-limiting step, but also other kinetic models may control the rate of biosorption, all of which may be operating simultaneously. The slope of the linear portion of the figure can be

Table 1
Kinetic model parameters for the biosorption of RR198 onto olive pomace.

t (°C)	k_1 (min^{-1})	q_e (mg g^{-1})	r_1^2	k_2 (g mg^{-1} min^{-1})	q_2 (mg g^{-1})	r_2^2	k_p (mg g^{-1} min$^{-1/2}$)	C (mg g^{-1})	r_p^2
20	4.66×10^{-2}	8.22	0.527	7.07×10^{-3}	41.96	0.999	5.07	12.97	0.997
30	4.06×10^{-2}	6.21	0.533	9.66×10^{-3}	42.59	0.999	3.69	20.98	0.957
40	2.56×10^{-2}	4.79	0.632	1.38×10^{-2}	42.80	0.999	2.76	27.03	0.978
50	3.09×10^{-2}	5.51	0.647	2.29×10^{-2}	43.75	0.999	2.09	30.67	0.913

used to derive values of the rate parameter, k_p, for the intraparticle diffusion, given in Table 1. The correlation coefficients (r_p^2) for the intraparticle diffusion model are also lower than that of the pseudo-second-order model but this model indicates that the biosorption of RR198 onto olive pomace may be followed by an intraparticle diffusion model up to 25 min.

3.7. Isotherm analysis

The results obtained for the biosorption of RR198 at different temperatures were analyzed in terms of Langmuir, Freundlich and D–R isotherm models.

The Langmuir equation is valid for monolayer coverage of biosorption of each molecule onto a completely homogeneous surface. According to this theory, once a dye molecule occupies a site, no further biosorption can take place at that site. Langmuir equation [50]:

$$\frac{1}{q_e} = \frac{1}{q_{max}} + \left(\frac{1}{q_{max}K_L}\right)\frac{1}{C_e} \tag{6}$$

where q_e and q_{max} are the equilibrium and monolayer biosorption capacities of the biosorbent ($mol\,g^{-1}$), respectively, C_e is the equilibrium dye concentration in the solution ($mol\,L^{-1}$) and K_L is the biosorption equilibrium constant ($L\,mol^{-1}$) related to the free energy of biosorption. Fig. 11 depicts a linear plot of $1/q_e$ versus $1/C_e$ for the biosorption of RR198 onto olive pomace. This plot suggests the monolayer coverage of dye at the outer surface of the biosorbent and shows the applicability of Langmuir model for the system at all temperatures studied. The maximum monolayer capacity of olive pomace for RR198 dye was found to be $1.08 \times 10^{-4}\,mol\,g^{-1}$ at $50\,°C$ and K_L values are in the range of 2.50×10^5 and $4.64 \times 10^4\,L\,mol^{-1}$ from the slope and intercept of the linear isotherm plots, respectively. Greater values of K_L indicate the affinity of biosorbent to investigated dye and imply strong bonding of dye anions. The dimensionless separation factor, R_L, was also evaluated using K_L values for all temperatures studied and calculated according to Eq. (7).

$$R_L = \frac{1}{1 + K_L C_o} \tag{7}$$

R_L values can be used for the interpretation of the sorption type and it was reported that, when $0 < R_L < 1$, the biosorption system is a favorable isotherm [51]. The values of R_L in the range of 7.80×10^{-3} to 4.22×10^{-3} indicate a favorable biosorption of RR198 dye onto olive waste.
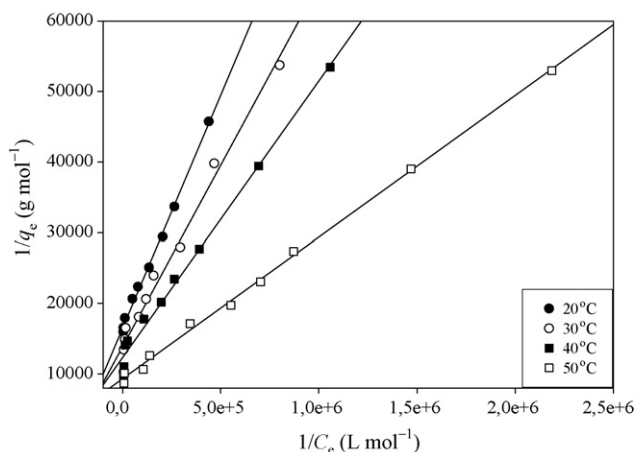

Fig. 11. Langmuir isotherm plots for the biosorption of RR198 onto olive pomace at different temperatures.
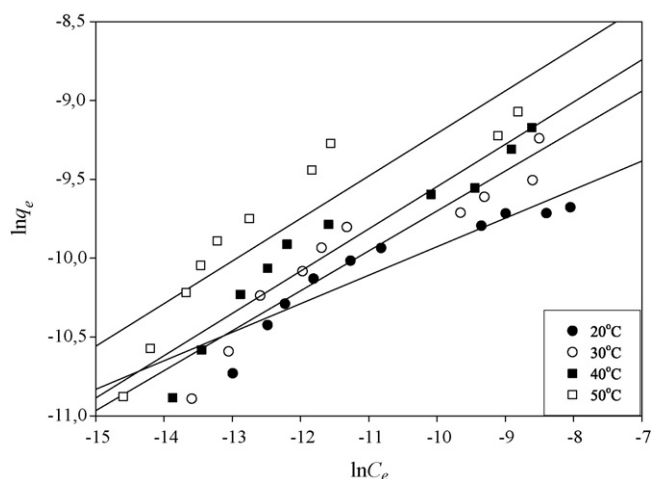

Fig. 12. Freundlich isotherm plots for the biosorption of RR198 onto olive pomace at different temperatures.

The Freundlich isotherm model provides no information on the monolayer biosorption capacity, in contrast to the Langmuir model. This model assumes that the biosorption process takes place on heterogeneous surfaces and Freundlich equation [52] is expressed as follows and Freundlich isotherm plots were shown in Fig. 12.

$$\ln q_e = \ln K_F + \frac{1}{n}\ln C_e \tag{8}$$

where K_F ($L\,mol^{-1}$) is a constant related to biosorption capacity of biosorbent and $1/n$ (dimensionless) is the biosorption intensity. K_F is a useful parameter for the biosorption capacity of dye in dilute concentrations of industrial effluents [38]. In this study, K_F values varied from 2.98×10^{-4} to $1.49 \times 10^{-3}\,L\,mol^{-1}$ for the biosorption of RR198 onto olive pomace. The values of K_F increased with an increase in the temperature indicated that the biosorption of RR198 onto olive pomace is favorable at higher temperatures. $1/n$ gives an indication of the favorability of biosorption and the values of $n > 1$ represent favorable biosorption condition [53]. n values were found high enough for olive pomace to be used for the removal of RR198 from aqueous solutions.

In order to distinguish between physical and chemical biosorption on the heterogeneous surfaces the equilibrium data are tested with the D–R isotherm model. According to the D–R isotherm [54] the characteristic biosorption curve is related to the porous structure of the sorbent. The D–R equation has the form [55]:

$$\ln q_e = \ln q_m - \beta \varepsilon^2 \tag{9}$$

q_m is the maximum biosorption capacity ($mol\,g^{-1}$), β is the activity coefficient related to the mean biosorption energy, R is the gas constant ($8.314\,kJ\,mol^{-1}$) and T is the absolute temperature (K) and ε is the Polanyi potential, equal to:

$$\varepsilon = RT \ln\left(1 + \frac{1}{C_e}\right) \tag{10}$$

D–R isotherm plots were presented in Fig. 13. The biosorption energy can be calculated by using β values as expressed in the following equation:

$$E = \frac{1}{(2\beta)^{1/2}} \tag{11}$$

The parameters related to each isotherm together with their correlation coefficients were presented in Table 2. The correlation coefficients in Table 2 suggest that the Langmuir model is more suitable for the experimental data in this study. Therefore the

Table 2
Isotherm model parameters for the biosorption of RR198 onto olive pomace.

t (°C)	Langmuir constants				Freundlich constants			Dubinin–Radushkevich				q_{exp} (mol g⁻¹)
	q_{max} (mol g⁻¹)	K_L (L mol⁻¹)	r_L^2	R_L	K_F (L mol⁻¹)	n	r_F^2	q_m (mol g⁻¹)	β (mol² kJ⁻²)	r_{D-R}^2	E (kJ mol⁻¹)	
20	6.05×10^{-5}	2.50×10^5	0.996	7.80×10^{-3}	2.98×10^{-4}	5.521	0.869	1.21×10^{-4}	1.22×10^{-3}	0.902	18.37	6.27×10^{-5}
30	7.21×10^{-5}	2.70×10^5	0.982	7.24×10^{-3}	7.72×10^{-4}	3.946	0.885	2.05×10^{-4}	1.36×10^{-3}	0.910	16.44	9.71×10^{-5}
40	8.12×10^{-5}	3.14×10^5	0.990	6.22×10^{-3}	1.05×10^{-3}	3.728	0.908	2.48×10^{-4}	1.34×10^{-3}	0.930	16.71	1.04×10^{-4}
50	1.08×10^{-4}	4.64×10^4	0.998	4.22×10^{-3}	1.49×10^{-3}	3.703	0.811	3.45×10^{-4}	1.29×10^{-3}	0.860	17.36	1.15×10^{-4}

Fig. 13. D–R isotherm plots for the biosorption of RR198 onto olive pomace at different temperatures.

biosorption of RR198 is seemed to be a monolayer sorption, and the biosorption takes place on a uniform surface.

3.8. Thermodynamic parameters

In order to investigate the effect of temperature on the biosorption of RR198 onto olive pomace and to understand the driving forces involved in biosorption process thermodynamic parameters such as standard Gibbs free energy change $\Delta G°$, standard enthalpy change $\Delta H°$ and standard entropy change $\Delta S°$ were determined and presented in Table 3. Temperature was changed from 293 to 323 K and K_L values were used to calculate the thermodynamic parameters in the following equations:

$$\Delta G° = -RT \ln K_L \tag{12}$$

$$\ln K_L = -\frac{\Delta G°}{RT} = -\frac{\Delta H°}{RT} + \frac{\Delta S°}{R} \tag{13}$$

The $\Delta S°$ and $\Delta H°$ values were calculated from the slope and intercept of a Van't Hoff plot (Fig. 14) of $\ln K_L$ versus $1/T$, respectively. The negative values of the free energy change suggest the biosorption of RR198 dye onto olive waste is spontaneous. This also emphasizes affinity of olive pomace for RR198. A positive value of enthalpy change, $\Delta H° = 15.524$ kJ mol⁻¹ demonstrates the endothermic nature of RR198 biosorption. A positive value of entropy change indicates an increase in degree of freedom of the sorbed dye molecules and characterizes some structural changes in sorbate and biosorbent [56]. This also reflects the release of water molecules due to the biosorption of large hydrated dye anions onto the biosorbent and attractive forces between oppositely charged groups [57].

3.9. Application to real wastewater

In order to evaluate the potential performance of the olive waste in real effluents, an optimized biosorption procedure was tested with model wastewater samples, with spikes, at predetermined optimum experimental conditions (pH: 2.0, biosorbent dosage:

Table 3
Thermodynamic parameters for the biosorption of RR198 onto olive pomace.

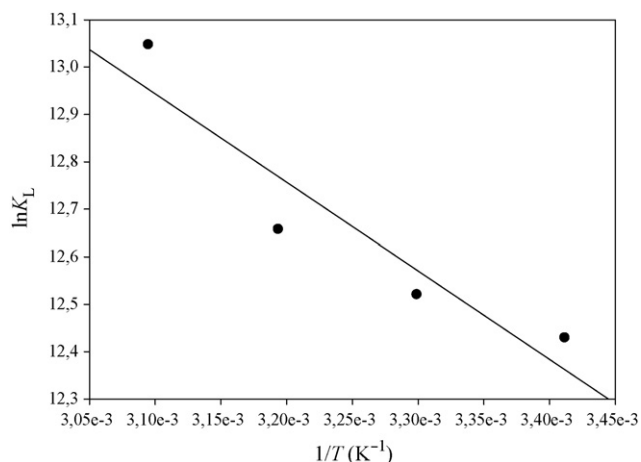| t (°C)	$\Delta G°$ (kJ mol⁻¹)	$\Delta H°$ (kJ mol⁻¹)	$\Delta S°$ (J K⁻¹ mol⁻¹)
20	−30.139	15.524	155.739
30	−31.689		
40	−33.246		
50	−34.803		

Fig. 14. The plot of $\ln K_L$ versus $1/T$ for the estimation of thermodynamic parameters.

Table 4
Some chemical characteristics of wastewater sample.

Parameters	Effluent quality
pH	2.24
Copper	46.86 mg L^{-1}
Lead	12.35 mg L^{-1}
Nickel	12.05 mg L^{-1}
Cadmium	14.83 mg L^{-1}
Iron	214.00 mg L^{-1}
Zinc	393.00 mg L^{-1}
Sodium	57.50 mg L^{-1}
Potassium	230.50 mg L^{-1}
Calcium	112.00 mg L^{-1}
Magnesium	182.00 mg L^{-1}

Table 5
The application of the proposed method in spiked samples.

Added RR198 (mg L^{-1})	q_e (mg g^{-1})	Biosorption yield (%)
5	0.99	59.40
50	14.11	84.66
100	27.12	81.36
150	41.38	82.76

$3.0\,\mathrm{g\,L^{-1}}$, volume of wastewater: 50 mL). Matrix effect on the biosorption capacity of waste biomass was investigated with spiked wastewater samples because the wastewater was not including this dye. Some characteristics of wastewater and biosorption results are presented in Tables 4 and 5, respectively. The biosorption capacity of olive pomace varied from 0.99 to 41.38 mg g^{-1} for the initial dye concentrations of 5.0 and 150.0 mg L^{-1}, respectively. In industrial wastewater spiked with RR198, the biosorption capacity of sorbent was slightly decreased due to the presence of interfering species in the wastewater. However, the results indicate that no significant matrix effect was observed, and that the proposed method could be successively applied to industrial wastewater containing RR198 dye.

4. Conclusions

1. This investigation shows that the olive pomace, an abundant and cost effective agricultural waste, can be used as biosorbent for the removal of RR198 textile dye from aqueous solutions.
2. The biosorption performance is affected from various parameters, i.e. pH, contact time, biosorbent concentration, temperature and initial dye concentration.
3. The kinetic and equilibrium data fitted well with the pseudo-second-order kinetic model and the Langmuir isotherm model,

respectively. The biosorption of RR198 onto olive pomace was found as monolayer biosorption on the homogeneous surface via chemisorption process.
4. The thermodynamic parameters show that the RR198 biosorption is spontaneous and endothermic.
5. The proposed biosorption system was successfully applied to real effluent spiked with RR198 dye.

References

[1] E. Aranda, I. Garcia-Romera, J.A. Ocampo, V. Carbone, A. Mari, A. Malorni, F. Sannino, A. De Martino, R. Capasso, Chemical characterization and effects on *Lepidium sativum* of the native and bioremediated components of dry olive mill residue, Chemosphere 69 (2007) 229–239.
[2] E. Mehmetli, O. Dogan, M. Tiris, N. Ciliz Kiran, G. Matuschek, Thermolysis product distribution of solid waste obtained from olive oil production, Clean 36 (2008) 315–319.
[3] Y. Kavdir, D. Killi, Influence of olive oil solid waste applications on soil pH, electrical conductivity, soil nitrogen transformations, carbon content and aggregate stability, Bioresour. Technol. 99 (2008) 2326–2332.
[4] I. Kula, M. Ugurlu, H. Karaoglu, A. Celik, Adsorption of Cd(II) ions from aqueous solutions using activated carbon prepared from olive stone by ZnCl$_2$ activation, Bioresour. Technol. 99 (2008) 492–501.
[5] F. Göğüş, M. Maskan, Air drying characteristics of solid waste (pomace) of olive oil processing, J. Food Eng. 72 (2006) 378–382.
[6] G. Rodriguez, A. Lama, R. Rodriguez, A. Jimenez, R. Guillen, J. Fernandez-Bolanos, Olive stone an attractive source of bioactive and valuable compounds, Bioresour. Technol. 99 (2008) 5261–5269.
[7] M. Konstantinou, K. Kolokassidou, I. Pashalidis, Sorption of Cu(II) and Eu(III) ions from aqueous solution by olive cake, Adsorption 13 (2007) 33–40.
[8] M.A. Martin-Lara, F. Pagnanelli, S. Mainelli, M. Calero, L. Toro, Chemical treatment of olive pomace: effect on acid–basic properties and metal biosorption capacity, J. Hazard. Mater. 156 (2008) 448–457.
[9] S. Doyurum, A. Celik, Pb(II) and Cd(II) removal from aqueous solutions by olive cake, J. Hazard. Mater. 138 (2006) 22–28.
[10] F. Banat, S. Al-Asheh, R. Al-Ahmad, F. Bni-Khalid, Bench-scale and packed bed sorption of methylene blue using treated olive pomace and charcoal, Bioresour. Technol. 98 (2007) 3017–3025.
[11] S.H. Gharaibeh, W.Y. Abu-El-Sha'r, M.M. Al-Kofahi, Removal of selected heavy metals from aqueous solutions using processed solid residue of olive mill products, Water Res. 32 (1998) 498–502.
[12] E. Malkoc, Y. Nuhoglu, M. Dundar, Adsorption of chromium(VI) on pomace—an olive oil industry waste: batch and column studies, J. Hazard. Mater. 138 (2006) 142–151.
[13] Z.A. Al-Anber, M.A.D. Matouq, Batch adsorption of cadmium ions from aqueous solution by means of olive cake, J. Hazard. Mater. 151 (2008) 194–201.
[14] F. Veglio, F. Beolchini, M. Prisciandaro, Sorption of copper by olive mill residues, Water Res. 37 (2003) 4895–4903.
[15] W.Y. Abu-El-Sha'r, S.H. Gharaibeh, S. Mahmoud, Removal of dyes from aqueous solutions using low-cost sorbents made of solid residues from olive-mill wastes (JEFT) and solid residues from refined Jordanian oil shale, Environ. Geol. 39 (2000) 1090–1094.
[16] G. Cimino, R.M. Cappello, C. Caristi, G. Toscano, Characterization of carbons from olive cake by sorption of wastewater pollutants, Chemosphere 61 (2005) 947–955.
[17] E.A. El-Sharkawy, A.Y. Soliman, K.M. Al-Amer, Comparative study for the removal of methylene blue via adsorption and photocatalytic degradation, J. Colloid Interface Sci. 310 (2007) 498–508.
[18] M. Uğurlu, A. Gürses, Ç. Doğar, Adsorption studies on the treatment of textile dyeing effluent by activated carbon prepared from olive stone by ZnCl$_2$ activation, Color. Technol. 123 (2007) 106–114.
[19] J.H. Ramirez, F.J. Maldonado-Hódar, A.F. Pérez-Cadenas, C. Moreno-Castilla, C.A. Costa, L.M. Madeira, Azo-dye Orange II degradation by heterogeneous Fenton-like reaction using carbon-Fe catalysts, Appl. Catal. B 75 (2007) 312–323.
[20] H. Keharia, H. Patel, D. Madamwar, Decolorization screening of synthetic dyes by anaerobic methanogenic sludge using a batch decolorization assay, World J. Microb. Biot. 20 (2004) 365–370.
[21] H. Lata, V.K. Garg, R.K. Gupta, Removal of a basic dye from aqueous solution by adsorption using *Parthenium hysterophorus*: an agricultural waste, Dyes Pigments 74 (2007) 653–658.
[22] A. Mittal, A. Malviya, D. Kaur, J. Mittal, L. Kurup, Studies on the adsorption kinetics and isotherms for the removal and recovery of Methyl Orange from wastewaters using waste materials, J. Hazard. Mater. 148 (2007) 229–240.
[23] N. Thinakaran, P. Baskaralingam, M. Pulikesi, P. Panneerselvam, S. Sivanesan, Removal of Acid Violet 17 from aqueous solutions by adsorption onto activated carbon prepared from sunflower seed hull, J. Hazard. Mater. 151 (2008) 316–322.
[24] J.P. Chen, S. Wu, K.H. Chong, Surface modification of a granular activated carbon by citric acid for enhancement of copper adsorption, Carbon 41 (2003) 1979–1986.
[25] G. Annadurai, R.S. Juang, D.J. Lee, Use of cellulose-based wastes for adsorption of dyes from aqueous solutions, J. Hazard. Mater. 92 (2002) 263–274.

[26] S.D. Khattri, M.K. Singh, Colour removal from dye wastewater using sugar cane dust as an adsorbent, Adsorp. Sci. Technol. 17 (1999) 269–282.

[27] F. Banat, S. Al-Asheh, L. Al-Makhadmeh, Evaluation of the use of raw and activated date pits as potential adsorbents for dye containing waters, Process Biochem. 39 (2003) 193–202.

[28] S. Tunali, A. Ozcan, Z. Kaynak, A.S. Ozcan, T. Akar, Utilization of the *Phaseolus vulgaris* L. Waste biomass for decolorization of the textile dye Acid Red 57: determination of equilibrium, kinetic and thermodynamic parameters, J. Environ. Sci. Health A 42 (2007) 591–600.

[29] G. Bayramoğlu, G. Çelik, M.Y. Arica, Biosorption of Reactive blue 4 dye by native and treated fungus *Phanerocheate chrysosporium*: Batch and continuous flow system studies, J. Hazard. Mater. 137 (2006) 1689–1697.

[30] W.T. Tsai, H.C. Hsu, T.Y. Su, K.Y. Lin, C.M. Lin, Removal of basic dye (methylene blue) from wastewaters utilizing beer brewery waste, J. Hazard. Mater. 154 (2008) 73–78.

[31] F.A. Pavan, E.C. Lima, S.L.P. Dias, A.C. Mazzocato, Methylene blue biosorption from aqueous solutions by yellow passion fruit waste, J. Hazard. Mater. 150 (2008) 703–712.

[32] M.H. Han, Y.S. Yun, Mechanistic understanding and performance enhancement of biosorption of reactive dyestuffs by the waste biomass generated from amino acid fermentation process, Biochem. Eng. J. 36 (2007) 2–7.

[33] S.W. Won, S.B. Choi, B.W. Chung, D. Park, J.M. Park, Y.S. Yun, Biosorptive decolorization of Reactive Orange 16 using the waste biomass of *Corynebacterium glutamicum*, Ind. Eng. Chem. Res. 43 (2004) 7865–7869.

[34] Z. Aksu, G. Karabayir, Comparison of biosorption properties of different kinds of fungi for the removal of Gryfalan Black RL metal-complex dye, Bioresour. Technol. 99 (2008) 7730–7741.

[35] R. Gong, Y. Ding, M. Li, C. Yang, H. Liu, Y. Sun, Utilization of powdered peanut hull as biosorbent for removal of anionic dyes from aqueous solution, Dyes Pigments 64 (2005) 187–192.

[36] R. Gong, Y. Ding, H. Liu, Q. Chen, Z. Liu, Lead biosorption and desorption by intact and pretreated *Spirulina maxima* biomass, Chemosphere 58 (2005) 125–130.

[37] G. Akkaya, A. Özer, Biosorption of Acid Red 274 (AR 274) on *Dicranella varia*: determination of equilibrium and kinetic model parameters, Process Biochem. 40 (2005) 3559–3568.

[38] E. Pehlivan, B.H. Yanık, G. Ahmetli, M. Pehlivan, Equilibrium isotherm studies for the uptake of cadmium and lead ions onto sugar beet pulp, Bioresour. Technol. 99 (2008) 3520–3527.

[39] D. Xu, X. Tan, C. Chen, X. Wang, Removal of Pb(II) from aqueous solution by oxidized multiwalled carbon nanotubes, J. Hazard. Mater. 154 (2008) 407–416.

[40] R. Herrero, P. Lodeiro, R. Rojo, A. Ciorba, P. Rodriguez, M.E. Sastre de Vicente, The efficiency of the red alga *Mastocarpus stellatus* for remediation of cadmium pollution, Bioresour. Technol. 99 (2008) 4138–4146.

[41] N. Ertugay, Y.K. Bayhan, Biosorption of Cr (VI) from aqueous solutions by biomass of *Agaricus bisporus*, J. Hazard. Mater. 154 (2008) 432–439.

[42] S. Lagergren, Zur theorie der sogenannten adsorption gelöster stoffe, Kungliga Svenska Vetenskapsakademiens, Handlingar 24 (1898) 1–39.

[43] Y.S. Ho, G. McKay, Kinetic models for the sorption of dye from aqueous solution by wood, Process Saf. Environ. Protect. 76 (1998) 183–191.

[44] W.J. Weber Jr., Adsorption theory, concepts and models, in: F.L. Slejko (Ed.), In Adsorption Technology: A Step by Step Approach to Process Evaluation and Application, Marcel Dekker, New York, 1985, pp. 1–35.

[45] N. Kannan, M.M. Sundaram, Kinetics and mechanism of removal of methylene blue by adsorption on various carbons-a comparative study, Dyes Pigments 51 (2001) 25–40.

[46] A. Ozcan, A.S. Ozcan, Adsorption of Acid Red 57 from aqueous solutions onto surfactant-modified sepiolite, J. Hazard. Mater. 125 (2005) 252–259.

[47] B. Chen, C.W. Hui, G. McKay, Film-pore diffusion modeling and contact time optimization for the adsorption of dyestuffs on pith, Chem. Eng. J. 84 (2001) 77–94.

[48] K.G. Bhattacharyya, A. Sharma, *Azadirachta indica* leaf powder as an effective biosorbent for dyes: a case study with aqueous Congo Red solutions, J. Environ. Manag. 71 (2004) 217–229.

[49] Y.S. Ho, G. McKay, Sorption of dye from aqueous solution by peat, Chem. Eng. J. 76 (1998) 115–124.

[50] I. Langmuir, The adsorption of gases on plane surfaces of glass, mica and platinum, J. Am. Chem. Soc. 40 (1918) 1361–1403.

[51] A. Özer, G. Akkaya, M. Turabik, The removal of Acid Red 274 from wastewater: Combined biosorption and biocoagulation with *Spirogyra rhizopus*, Dyes Pigments 71 (2006) 83–89.

[52] H.M.F. Freundlich, Über die adsorption in lösungen, Z. Phys. Chem. 57 (1906) 385–470.

[53] B.H. Hameed, Equilibrium and kinetic studies of methyl violet sorption by agricultural waste, J. Hazard. Mater. 154 (2008) 204–212.

[54] T. Akar, A.S. Ozcan, S. Tunali, A. Ozcan, Biosorption of a textile dye (Acid Blue 40) by cone biomass of *Thuja orientalis*: Estimation of equilibrium, thermodynamic and kinetic parameters, Bioresour. Technol. 99 (2008) 3057–3065.

[55] M.M. Dubinin, L.V. Radushkevich, Proc. Acad. Sci. U.S.S.R.: Phys. Chem. Sect. 55 (1947) 331–333.

[56] K. Vijayaraghavan, Y.S. Yun, Biosorption of C.I. recative Black 5 from aqueous solution using acid-treated biomass of brown seaweed *Laminaria sp*, Dyes Pigments 76 (2008) 726–732.

[57] D. Bilba, D. Suteu, T. Malutan, Removal of reactive dye brilliant red HE-3B from aqueous solutions by hydrolyzed polyacrylonitrile fibres: equilibrium and kinetics modeling, Cent. Eur. J. Chem. 6 (2008) 258–266.